Research Paper

Experimental Diagnostic of Cavitation Flow in the Centrifugal Pump Under Various Impeller Speeds Based on Acoustic Analysis Method

Ahmed Ramadhan AL-OBAIDI

Faculty of Engineering, Department of Mechanical Engineering, Mustansiriyah University
Baghdad, Iraq; e-mail: ahmedram@uomustansiriyah.edu.iq

Condition monitoring in a centrifugal pump is a significant field of study in industry. The acoustic method offers a robust approach to detect cavitations in different pumps. As a result, an acoustic-based technique is used in this experiment to predict cavitation. By using an acoustic technique, detailed information on outcomes can be obtained for cavitation detection under a variety of conditions. In addition, various features are used in this work to analyze signals in the time domain using the acoustic technique. A signal in the frequency domain is also investigated using the fast Fourier method. This method has shown to be an effective tool for predicting future events. In addition, this experimental investigation attempts to establish a good correlation between noise characteristics and cavitation detection in a pump by using an acoustic approach. Likewise, it aims to find a good method for estimating cavitation levels in a pump based on comparing and evaluating different systems.

Keywords: experimental analysis; impeller speed; cavitation; acoustic signals.

1. Introduction

Various pump industries have become increasingly interested in the phenomenon of cavitation. Several types of hydraulic machinery may be affected by cavitation. This includes all types of pumps and turbines for water (Nelik, 1999; Al-Obaidi, 2018; 2019a; 2019b; Spraker, 1965). A variety of factors contribute to this problem (Girdhar, Moniz, 2005; Arnold, Stewart, 1999; Gautam, 2012). As a consequence, all systems become noisier (Lobanoff, Ross, 2013; Liu, 2014; Anderson *et al.*, 2014). To detect cavitation in a pump, experimental acoustic signals are analyzed, and a variety of frequency ranges are studied (Karassik, McGuire, 1998; Beebe, 2004; Alfayez *et al.*, 2005). The performance of pumps has been investigated by many researchers using a variety of monitoring techniques. For example, noise was used to investigate cavitation as an indicator of a pump's performance (Chudina, 2003). Cavitation occurs in the inlet pump because of several undesired influences such as performance drop, pitting, erosion, and pump damage. The study analyzes acoustic signatures at various frequencies under different conditions. A higher frequency range is found to enhance cavitation at high mass flow.

Both vibrations and noise were used to monitor cavitation (Černetič *et al.*, 2008). Pumps were used with a semi-open impeller and a closed impeller, both of which have six blades. Each pump was studied separately for cavitation. The results indicated that every pump has a variety of noise and vibration spectra with many different types of frequencies. In addition, the results showed that the alteration levels for noise and vibration were around 10 to 15 dB with and without cavitation. The vibration method was used to investigate faults in the pump (Albraik *et al.*, 2012). The flow rate was 30 m^3/h, the head was 55 m, and the impeller speed was 2900 rpm for a closed impeller pump. Gradually closing the discharge valve and keeping the suction valve open showed that the net positive suction head available (NPSHA) was related to the net positive suction head required (NPSHR). In their study, NPSHR increased with the mass flow. The results also revealed that the vibration level increased as the mass flow grew.

Farokhzad *et al.* (2013) conducted a study on relationship between vibration and fault in a pump at various conditions. Two different configurations were found to be faulty: a faulty seal and a broken impeller. The authors found that significant alteration in vibration tendencies occurred with fault. Čudina (2003) investigated cavitation using the sound signal and investigated the sound level at a variety of discharge conditions. The results showed that the sound level increased as cavitation became fully developed. The noise in the pump increased or decreased depending on the mass flow and pump speed. Also, instability can happen in the pump due to cavitation, causing pump deterioration performance, pitting in material, and erosion. Čudina and Prezelj (2009) examined cavitation by studying frequency of discrete audible spectra. The results found that the discrete frequency spectrum of audible noise was linked with cavitation in the pump. Moreover, the spectra frequency level peak augmented as the cavitation inception grew, and the maximum value occurred during the cavitation process.

Based on the above literature, it can be noticed that there is a lack of details connected to using various frequency range analyzes to detect cavitation phenomenon. It is essential that cavitations are investigated when the pump performs at high range conditions, for instance, at various mass flow rates and pump speeds. Using condition monitoring type acoustic approach has different advantages. It is easily recorded, evading safety dangers and the need for different ranges of temperature acoustic devices with their connected complications of mounting. The most significant disadvantage of the acoustic approach is that the sur-

rounding noise tends to contaminate the microphone (Ramroop *et al.*, 2001; Sakthivel *et al.*, 2010; Jones *et al.*, 2006; Grist, 1998; Kamiel, 2015). In this experimental work, the methodology used contains a variety of steps, as shown in Fig. 1.

2. Centrifugal pump experimental test rig

Figure 2 illustrates a flow loop system with a pump and sensors; clear PVC (polyvinyl chloride) pipes were used. In addition, the tank was made of plastic. A pump experimental test rig construction consisted of different significant stages. Designing a flow-loop pumping system was the first step. In the second stage, all requirements, such as installing the entire piping system, were conducted. A pressure transducer microphone, water flowmeter, and other equipment were also identified as part of the loop installation sensors.
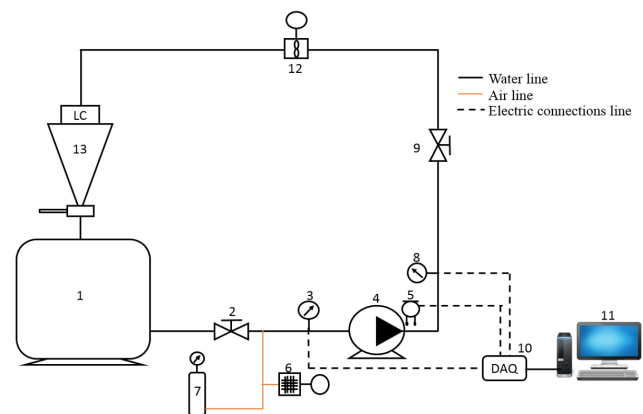

Fig. 2. Experimental setup components: 1 – water tank; 2 – suction valve; 3 – suction pressure transducer; 4 – centrifugal pump; 5 – microphone; 6 – air flowmeter; 7 – air supply; 8 – discharge pressure transducer; 9 – discharge value; 10 – data acquisition system; 11 – PC; 12 – water flowmeter; 13 – hopper.

2.1. Time domain conventional statistical analysis

Peak value analysis

It is a significant statistical parameter to calculate the peak signal.

RMS value

The given equation defines the RMS value:

$$\text{RMS} = \sqrt{\frac{1}{N} \sum_{i=1}^{N} x_i^2}, \tag{1}$$

where N and x_i represent the total elements' number and the element signal.

Value of peak-to-peak

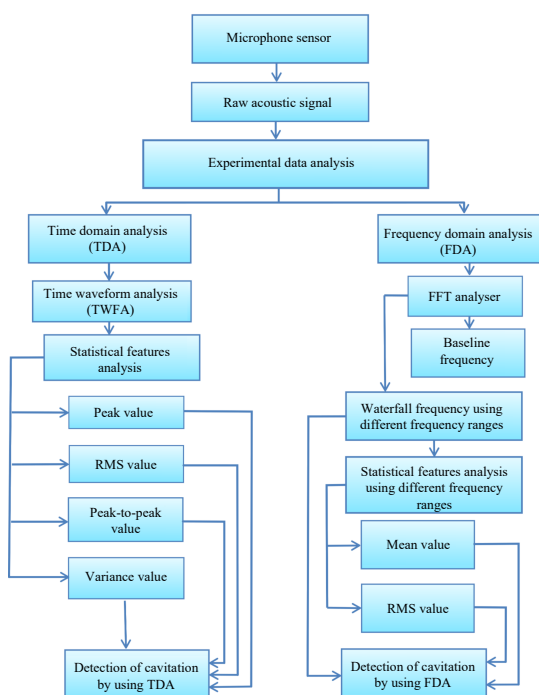This is the third statistical parameter used in this work.

Fig. 1. Flow chart analysis of acoustic data processing.

Variance value

Variance value can be calculated using Eq. (2):

$$\text{Variance} = \frac{\sum \left(x_i - \overline{\overline{x}} \right)^2}{N-1}, \tag{2}$$

where $\overline{\overline{x}}$, x_i, and N are the total of elements, the set of elements, and the elements' mean values, respectively.

Frequency conventional analysis

The fast Fourier transform (FFT) is broadly employed to convert the different types of signals from the time analysis into the frequency-domain analysis. The outcome of the FFT offers various amplitudes of signals, and the FFT can be written as follows:

$$F(\omega) = \int\limits_{-\infty}^{\infty} X(t) e^{j2\pi * ft} \, \mathrm{d}t. \tag{3}$$

The inverse function of the FFT is defined as:

$$X(t) = \int\limits_{-\infty}^{\infty} F(\omega) e^{j2\pi * ft} \, \mathrm{d}\omega, \tag{4}$$

$$j = \sqrt{-1}, \tag{5}$$

$$\omega = 2\pi f, \tag{6}$$

where

$$e^{j2\pi * ft} = \cos 2\pi ft + \sin 2\pi ft. \tag{7}$$

$X(t)$ and $F(\omega)$ are the time signals and frequency domain, respectively.

Mean value analysis

The mean value is calculated using the following equation:

$$\mu = \frac{1}{N} \sum_{i=0}^{N-1} x_i. \tag{8}$$

The x, x_i, and N, are the total of elements, the set of elements, and the elements' mean values.

Root mean square analysis

From the frequency domain, it can be calculated by the root mean square (RMS) (ANDERSON *et al.*, 2014). The value of the H-NPSHR curve in the pump was provided by its manufacturer and the value of NPSHA, calculated based on varying conditions, is as follows:

$$\text{NPSHA} = \frac{P_{\text{atm}} + P_s}{\rho g} + \frac{V^2}{2g} - \frac{P_v}{\rho g} - H_i, \tag{9}$$

where P_{atm} – atmospheric air pressure [Pa], P_i – inlet pressure [Pa], V – water velocity in pipes [m/s], P_v – the pressure of water vapor [Pa].

3. Instantaneous outlet pressure (hydrostatic pressure) analysis

Figure 3 represents the signals of the outlet pressure (hydrostatic pressure) for various mass flows ranging from 152 to 378 l/min with an impeller speed of 2755 rpm in the centrifugal pump. The outlet pressure signals are changed when the mass flow changes, and the pressure magnitude decreases as the mass flow increases. This resulted from both mechanical and hydraulic losses as well as cavitation conditions. In the next part of this experiment, additional investigations will be necessary to detect cavitation.

Figure 4 describes the tendency of minimum, RMS, mean, and peak features for the amplitude of signals of outlet pressure. It is obvious that the features with the growing flow in the pump all follow a downward continuous tendency because of the same reasons stated before. The tendency for entire features rapidly reduces as the pump works at the mass flow greater than 350 l/min due to the high interaction flow in the impeller and volute parts as well as the cavitation occurrence.

Figure 5 illustrates the pump head measurements at various mass flows. According to experiments, the pump head decreases as the flow increases. Pressure alterations occur when there is interaction flow in the impeller due to the distribution pressure being nonuniform in the volute as well as when there is cavitation.

When it comes to determining normal and cavitation conditions, the NPSH is an influential parameter in the performance of the pump. Figure 6 describes the NPSHA and the NPSHR. The pump's flow in the pump can be altered by gradually throttling the valve at discharge suction and keeping the valve at the suction part fully open.

As can be seen, there are various regions of cavitation. In the first one, at low flow, no cavitation occurs in this area. At mass flow greater than 350 l/min, the cavitation starts to occur and an intersection between both curves has already formed, as shown in this figure. Furthermore, cavitation occurs more frequently at flow rates greater than 300 l/min. Also, it is observed that cavitation occurs between flow rates of 300 and greater than 350 l/min.

4. Acoustic analysis signal in the time domain

In this experimental measurement study, cavitation is investigated at a variety of conditions using various types of features in the time analysis domain. Figure 7 illustrates the acoustic signals in time analysis waves. It is noted that the flow is lower than the flow of 300 l/min. As can be seen, there is no alteration in acoustic amplitude characteristics. The important change in signals occurs at a rate greater than 350 l/min, due to the interaction flow in the volute
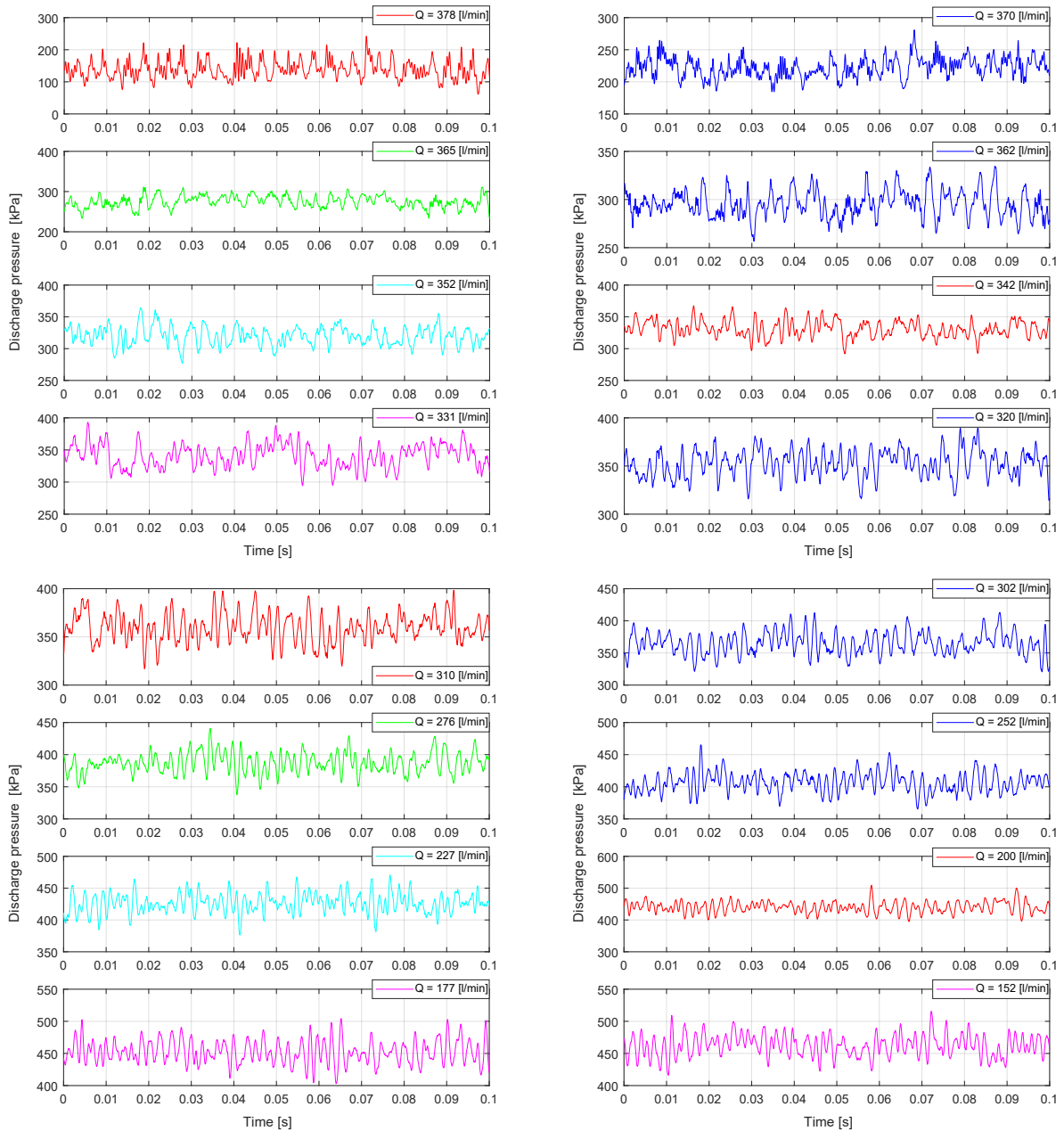
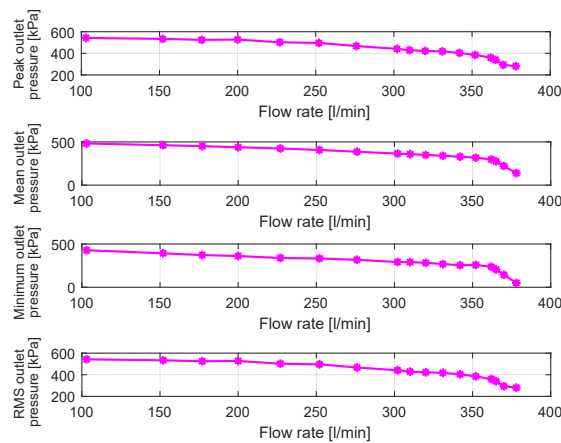Fig. 3. Various signals of outlet pressure in time analysis.

Fig. 4. Tendency of the peak, mean, minimum, and RMS features for the signals of outlet pressure.
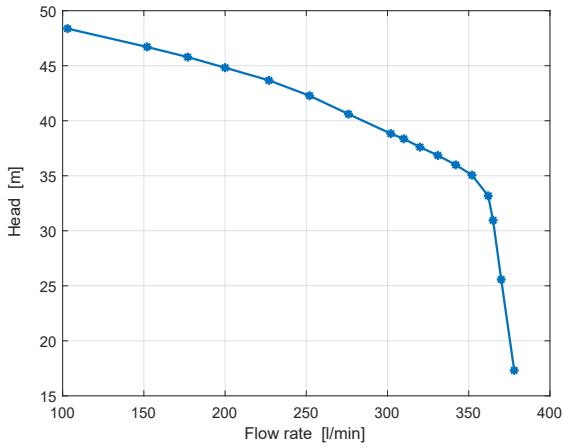
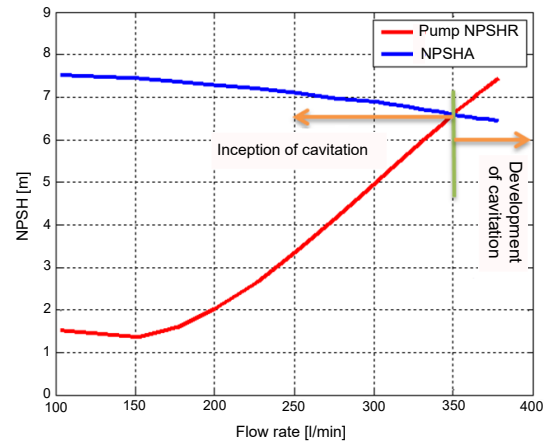Fig. 5. Pump head at different conditions.

Fig. 6. Characteristics of NPSH with and without cavitation.
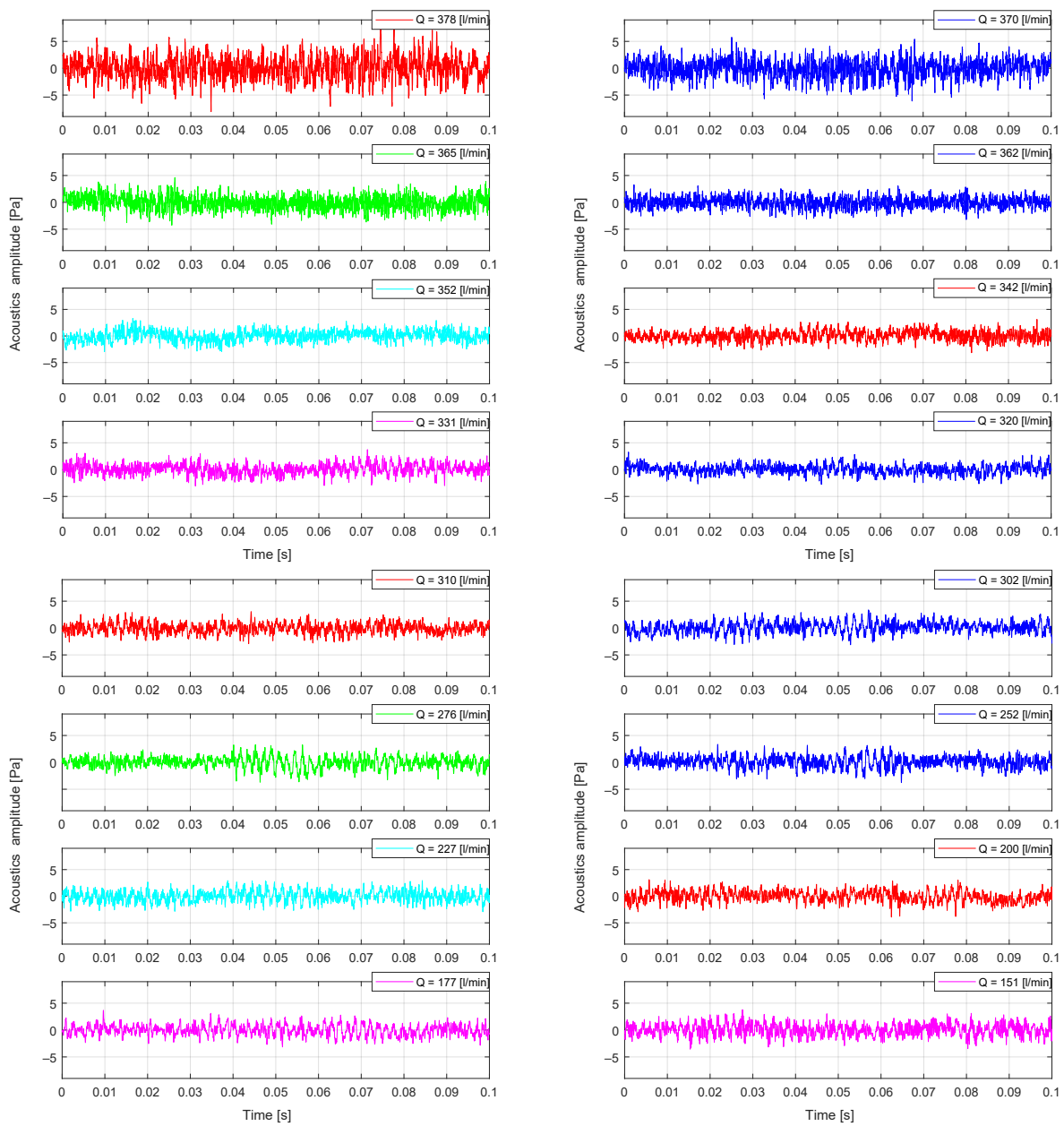

Fig. 7. Acoustic signature in time analysis domain.

and impeller and the cavitation resulting in an NPSHR value higher than NPSHA.

Further analysis conducted to find the relationship between the acoustic signature and the occurrence of cavitation is presented in the next part.

5. Acoustic signals analysis using features

Figure 8a shows the peak and RMS values of microphone signal to investigate cavitation. Because of the inner recirculation flow, there is increased hydraulic noise when the pump runs with a lower flow than the designation flow. Likewise, as the pump functions at a flow greater than 300 l/min, the noise level increases because of additional hydraulic noise, flow turbulence, and the cavitation process. However, when flow increases a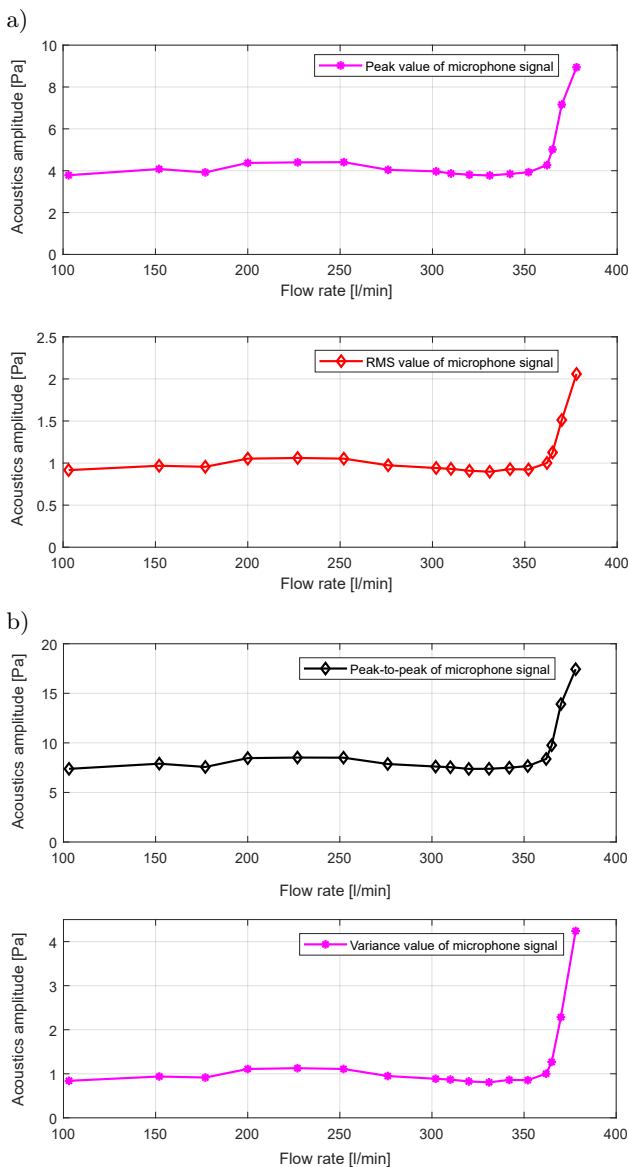bove 350 l/min, the signature of the acoustic signal rapidly increases. The bubbles collapse, consequently altering noise that leads to the NPSHR being higher than the NPSHA due to the cavitation process.

Figure 8b shows an acoustic signature analysis for additional investigation of the acoustic signature using various statistical values of peak-to-peak feature and variance feature. Figure 8b shows that the above features tend to have a similar tendency to those in Fig. 8a. Since the flow inside the pump changes at different range conditions, the noise level increases. According to this observation, the cavitation phenomenon in the pump is highly affected by the mass flow. Furthermore, using the above feature can provide a good indicator of cavitation.

In this experiment, the purpose is to examine the cavitation process in a pump under various conditions. The 3D figure below explains the connection between various parameters. This figure compares acoustic signals in the frequency analysis. It is demonstrated how the acoustic signals vary in the pump. Figure 9a describes these signals in the low-frequency range of $0\,\text{Hz} - 1\,\text{kHz}$. Based on the results, the acoustic signal did not change when the pump operated below $350\,\text{l/min}$. However, the significant alteration in the
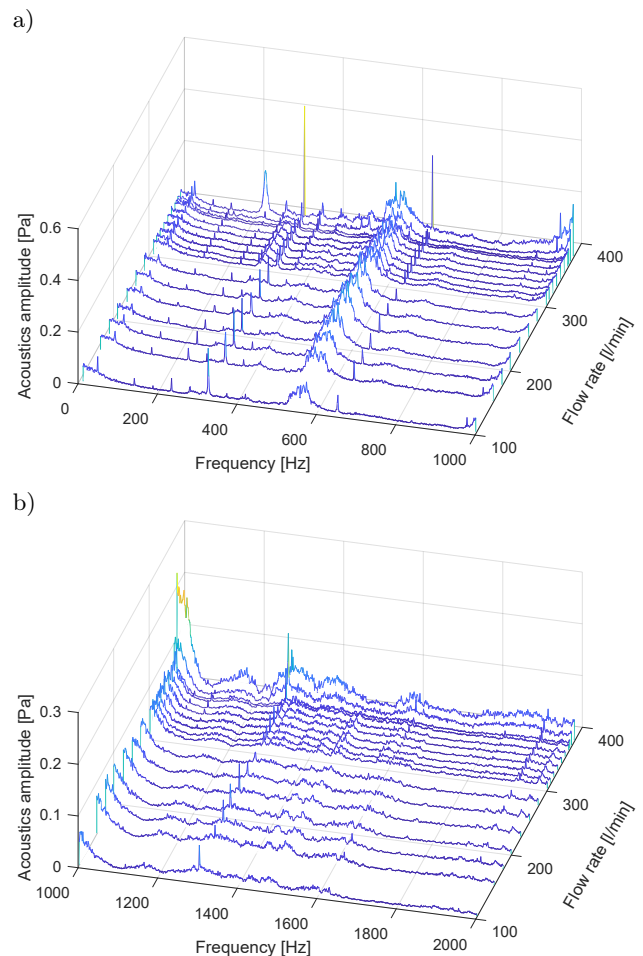
a)

b)

Fig. 8. Tendencies of the acoustics signature using peak, RMS, peak-to-peak, and variance signature features.

a)

b)

Fig. 9. Amplitude acoustic analysis at the range of frequency: a) $0\,\text{Hz} - 1\,\text{kHz}$; b) 1–2 kHz.

acoustic level was observed for the pump operating with 350 l/min and greater. Due to the interaction flow between the volute and impeller as well as cavitation, in general, the noise level increases. The dominant frequencies in the pump are the blade passing frequency of 229.5 Hz, the rotation impeller frequency of 45.9 Hz, and harmonics.

6. Acoustic signals in the frequency analysis domain

Figure 9b shows the signals in the frequency range from 1 kHz to 2 kHz. Based on this frequency range, the results revealed a slight alteration in amplitude signals as the pump operated at less than 350 l/min; nevertheless, a quick increase in amplitude signals is indicated under the flow greater than 350 l/min. Due to the occurrence of cavitation, the NPSHA was smaller than the NPSHR. Also, it was observed that the blade passing frequency (BPF) and rotational frequency (RF) dominated in this frequency range.

Figure 10 shows two ranges of frequencies: a) 2 to 10 kHz and b) 10 to 15 kHz. The flow rate of the pump
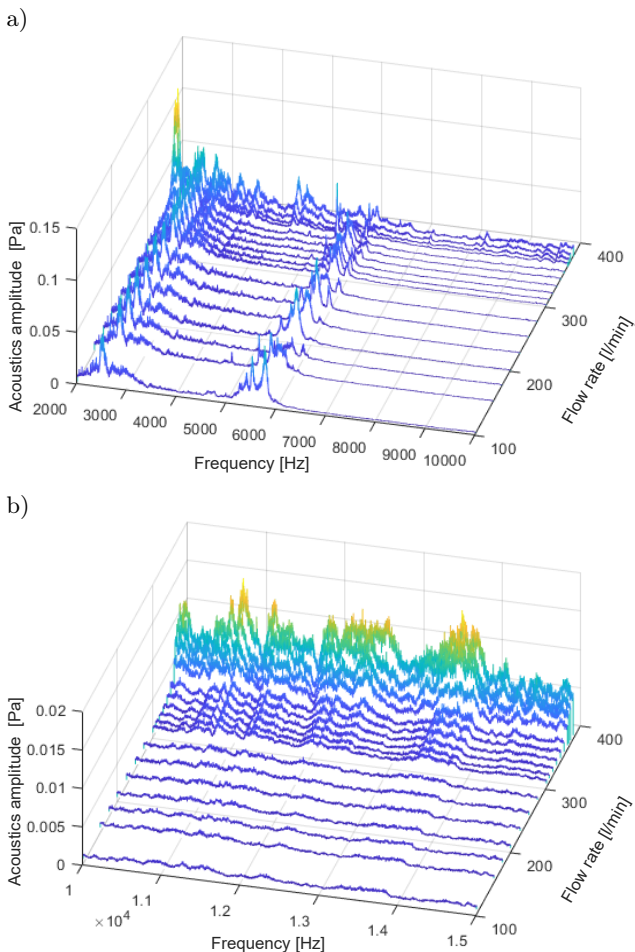
a)

b)

Fig. 10. Amplitude acoustic analysis at the frequency ranges: a) 2–10 kHz; b) 10–15 kHz.

is less than 350 l/min. No alteration in the acoustic signal levels is noted. A significant rise is detected when the flow exceeds 350 l/min. Cavitation growth occurs at high mass flow rates. As a result of cavitation, the noise level increases under high flow. The frequency range from 10 to 15 kHz was also effective in diagnosing cavitation.

6.1. Acoustic signals in the frequency analysis using the mean feature

Figure 11 illustrates acoustic amplitude signals mean value at the frequency ranges of 0 Hz – 1 kHz, 1–2 kHz, 2–10 kHz, and 10–15 kHz. It is revealed that using the mean feature, there is no important alteration as the pump works under smaller than the design flow. Nevertheless, it is noted that the quick rise in acoustic level takes place under the flow greater than 350 l/min because of the cavitation occurrence. Also, the NPSHR is greater than the NPSHA in this case. The result indicates that using the mean value in the frequency domain offers a good approach to analyze cavitation.
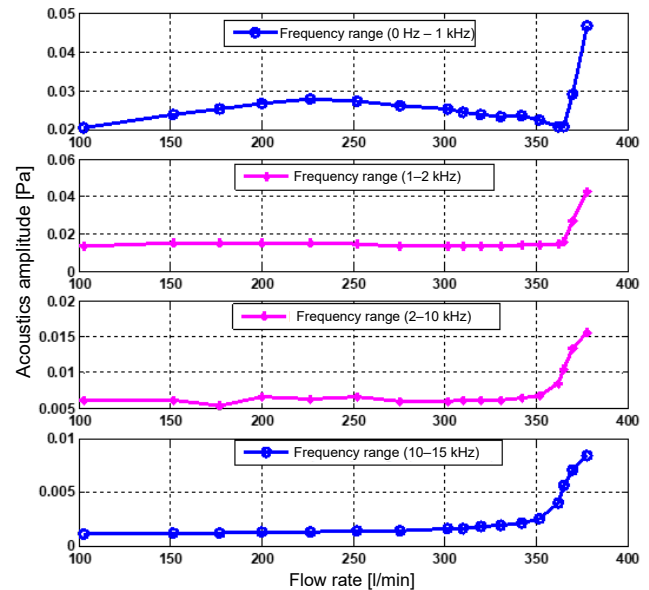

Fig. 11. Mean feature analysis in the frequency range between 0 Hz and 15 kHz.

6.2. Using the RMS feature in the frequency analysis domain

Figure 12 describes the acoustic signal analysis using the RMS feature for frequency ranges from 0 Hz to 15 kHz. All curves in this figure have the same tendency as the acoustic mean feature in Fig. 11. The amplitudes of acoustic signals rapidly increase at a flow higher than 350 l/min for all ranges of frequencies. Also, the results show that the differences in ampli-
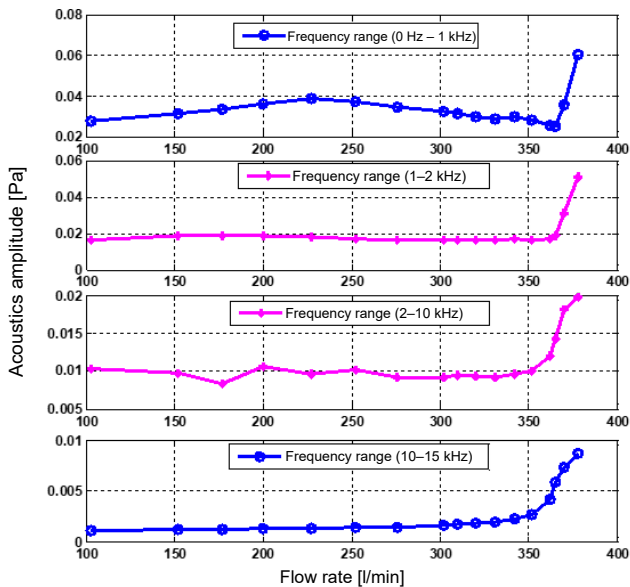
Fig. 12. RMS feature at the frequency range between 0 Hz
and 15 kHz.

tudes of acoustic in frequency analysis at a variety of
mass flows and frequency ranges agreed with cavita-
tion characteristics in Fig. 6.

7. Influence of impeller speed on the cavitation occurrence

Figure 13 illustrates maximum statistical feature
values. It is obvious that these values under an im-
peller speed of 2755 rpm are significantly higher than
in other three remaining impeller speeds of 2610, 2320,
and 2030 rpm. The peak value of the impeller speed of
2755 rpm is higher by about 13.4%, 15.5%, and 35.59%
compared to 2610, 2320, and 2030 rpm, respectively.
Similarly, the RMS value is higher by around 11.8%,
29.95%, and 52.6%, the peak-to-peak value by about
13.1%, 13.5%, and 33.3%, and the variance value by
around 16.7%, 42.2%, and 75.89%, as summarized in
Tables 1 and 2.

Table 1. Summary of the maximum statistical feature re-
sults for the acoustic amplitude at different impeller speeds.

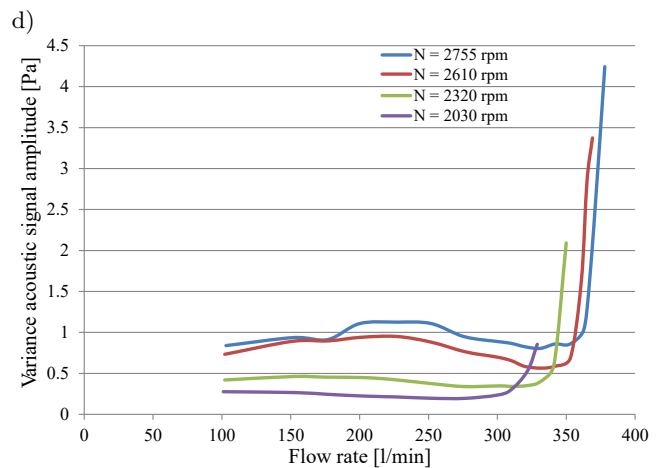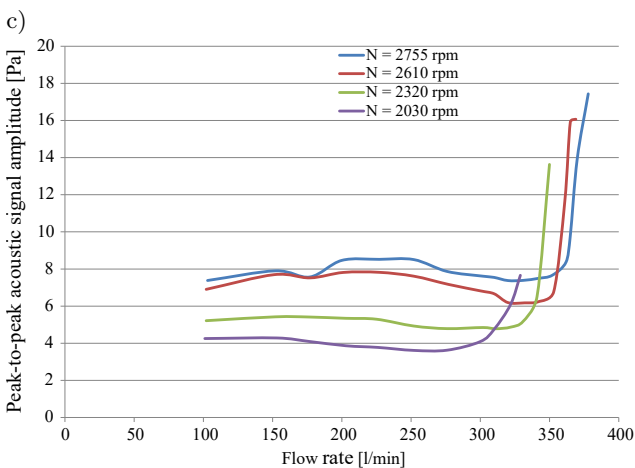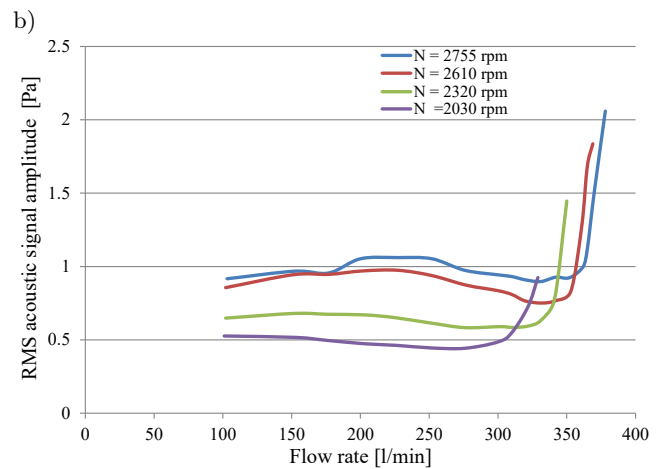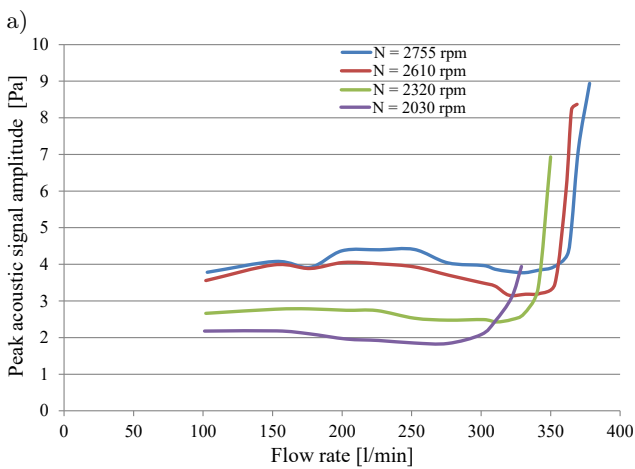| Impeller speed [rpm]	Peak [Pa]	RMS [Pa]	Peak-to-peak [Pa]	Variance [Pa]
2755	0.045	0.043	0.016	0.0085
2610	0.039	0.036	0.016	0.0084
2320	0.035	0.027	0.011	0.0063
2030	0.023	0.016	0.0065	0.0034

Fig. 13. Comparison of the results of various features at various impeller speeds.

Table 2. Summary of the minimum statistical feature results for the acoustic amplitude at different impeller speeds.

Impeller speed [rpm]	Peak [Pa]	RMS [Pa]	Peak-to-peak [Pa]	Variance [Pa]
2755	3.79	0.92	7.39	0.85
2610	3.56	0.86	6.92	0.74
2320	2.67	0.65	5.22	0.43
2030	2.18	0.53	4.26	0.28

Figure 14 describes the signal investigation in the frequency analysis using the mean feature at various mass flows and impeller speeds for the frequency range from 0 Hz to 15 kHz.

The results indicate that the mean feature for the pump speed of 2755 rpm is higher than for N = 2610, N = 2320, and N = 2030 rpm. Similarly, it is noted that the impeller speed is related to the increase of acoustic signal amplitude. The mean values increase as the pump speed increases, as listed in Table 3. A comparison of results for the minimum mean acoustic value is presented in Table 4.

Table 3. Comparison results for the maximum mean acoustic values.

Impeller speed [rpm]	Mean value 0 Hz – 1 kHz [Pa]	Mean value 1–2 kHz [Pa]	Mean value 2–10 kHz [Pa]	Mean value 10–15 kHz [Pa]
2755	0.047	0.043	0.016	0.0085
2610	0.039	0.036	0.0158	0.0084
2320	0.035	0.027	0.011	0.0063
2030	0.023	0.016	0.0065	0.0034

Table 4. Comparison results for the minimum mean amplitude features.

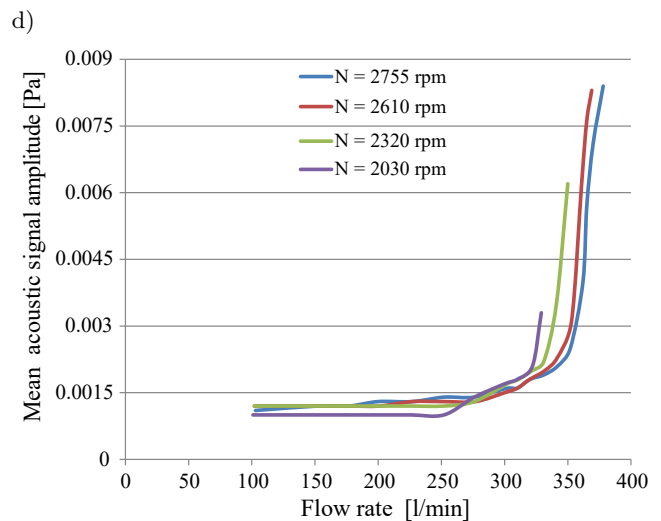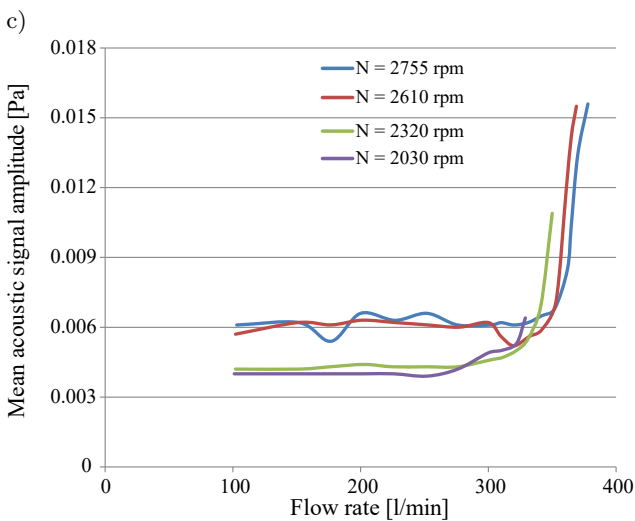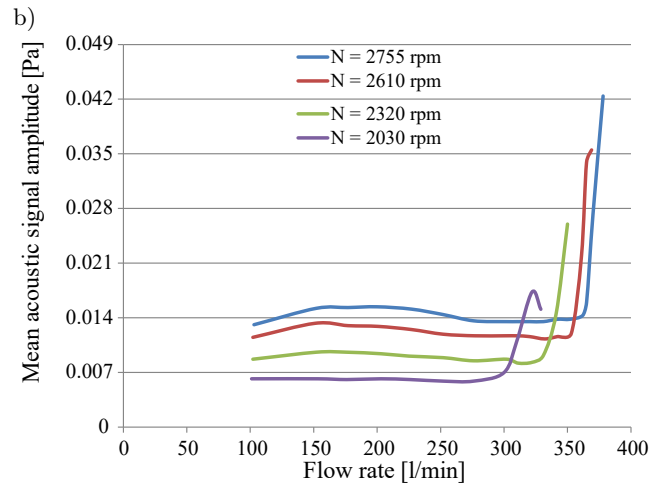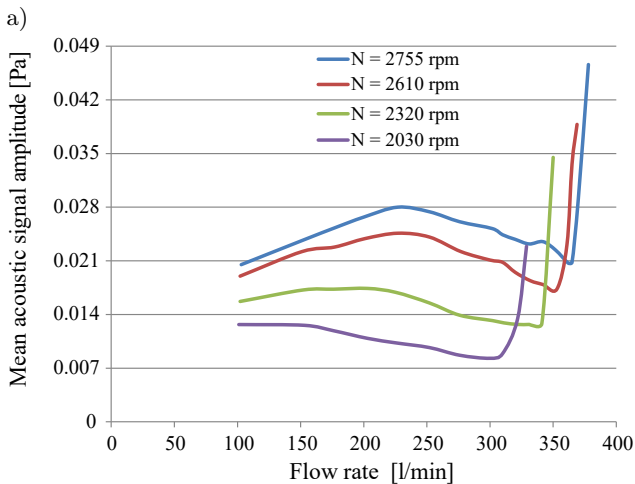| Impeller speed [rpm]	Mean value 0 Hz – 1 kHz [Pa]	Mean value 1–2 kHz [Pa]	Mean value 2–10 kHz [Pa]	Mean value 10–15 kHz [Pa]
2755	0.021	0.014	0.0062	0.0012
2610	0.0189	0.012	0.0058	0.0011
2320	0.016	0.0088	0.0043	0.00105
2030	0.013	0.0063	0.0041	0.00103

Fig. 14. Results comparison for mean feature at the frequency range between 0 Hz and 15 kHz.

Figure 15 illustrates the RMS analysis at the range frequency from 0 Hz to 15 kHz. The results reveal that the RMS value for the pump speed of 2755 rpm is significantly greater than for the cases with N = 2610, N = 2320, and N = 2030 rpm. It is also observed that the maximum and minimum values of the RMS features increase as the impeller speed increases, as listed in Tables 5 and 6.

Table 5. Comparison of maximum value results of the RMS feature.

Impeller speed [rpm]	Maximum value 0 Hz – 1 kHz [Pa]	Maximum value 1–2 kHz [Pa]	Maximum value 2–10 kHz [Pa]	Maximum value 10–15 kHz [Pa]
2755	0.061	0.052	0.019	0.009
2610	0.048	0.043	0.018	0.008
2320	0.047	0.031	0.014	0.007
2030	0.033	0.023	0.009	0.004

Table 6. Comparison of maximum value results of the RMS feature.

Impeller speed [rpm]	Minimum value 0 Hz – 1 kHz [Pa]	Minimum value 1–2 kHz [Pa]	Minimum value 2–10 kHz [Pa]	Minimum value 10–15 kHz [Pa]
2755	0.026	0.017	0.009	0.0014
2610	0.022	0.014	0.0085	0.0013
2320	0.017	0.008	0.0065	0.00125
2030	0.011	0.006	0.0055	0.00101

8. Conclusions

The following outcomes are derived in this investigation studying the influence of different mass flows and impeller speeds using acoustic signals on detecting cavitation occurrence. Time-domain analysis of the acoustic signal's amplitude in time by various features can provide a good indication of cavitation. The results
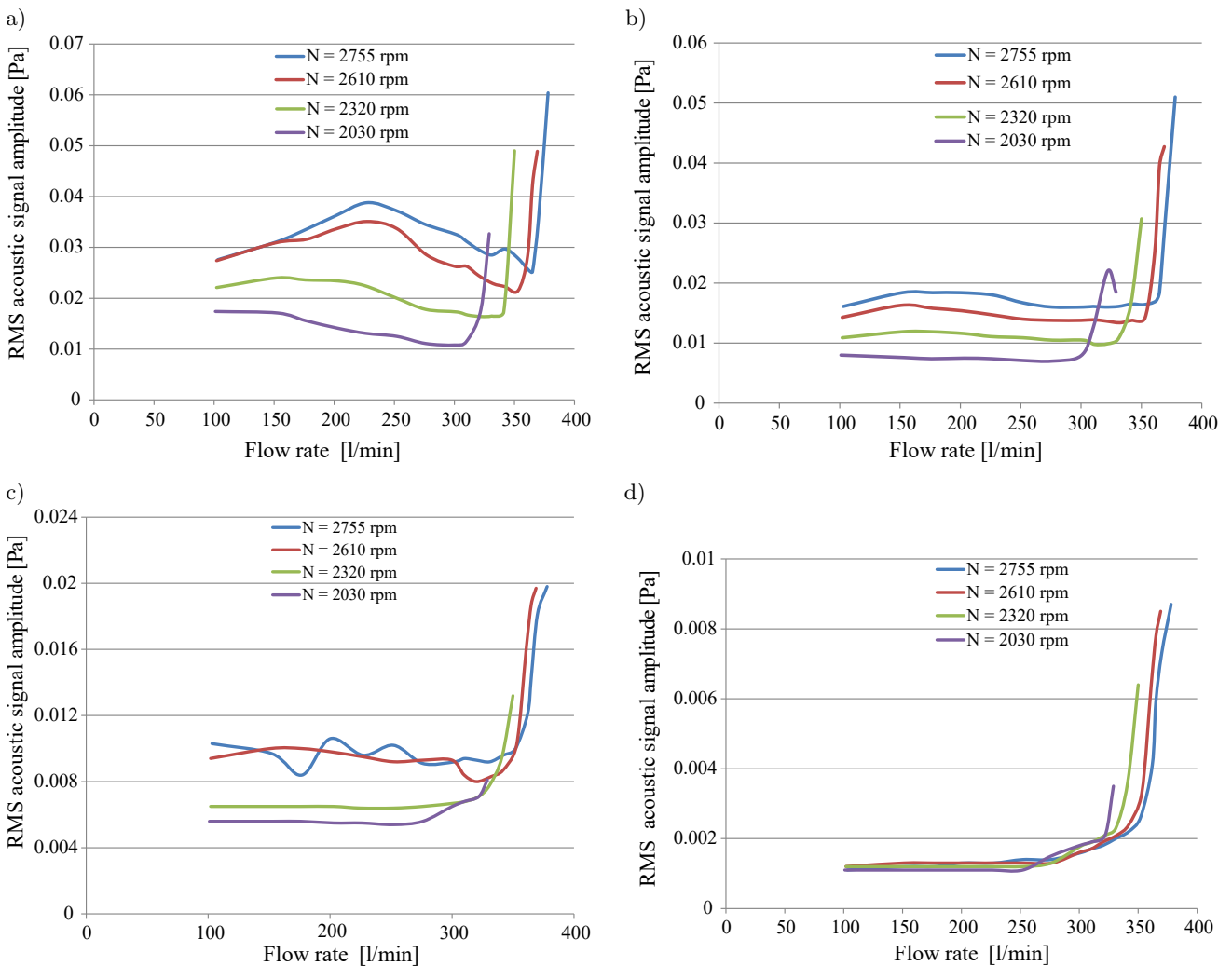

Fig. 15. RMS features comparison at the frequency range from 0 Hz to 15 kHz.

found that the value of the acoustic signal amplitude increased or decreased directly with the flow range in the pump. Acoustic signals in the time domain showed that the level of acoustic signal increased as the pump worked at the occurrence of cavitation. Also, studying the acoustic amplitude in frequency analysis is a satisfactory approach to study changes in cavitation. The dominant frequencies in the pump are the blade passing frequency, the rotation frequency, and its harmonics. Various frequency ranges offer good indications of determining cavitation by examining the amplitude of the acoustic signal in the frequency analysis. The results showed that mean and RMS features in the frequency analysis effectively detect cavities. The study of the acoustic signal amplitude under a variety of experimental tests displayed a good agreement with cavitation characteristics demonstrated in the NPSH plot. Furthermore, the result comparison in both time and frequency analyzes revealed that both mean and RMS features under an impeller speed of 2755 rpm are significantly greater than in other experimental cases. According to this study's experimental results, the acoustic method effectively detects the various levels of cavitation.

Acknowledgments

References

1. Albraik A., Althobiani F., Gu F., Ball A. (2012), Diagnosis of centrifugal pump faults using vibration methods, [in:] *Journal of Physics: Conference Series, 25th International Congress on Condition Monitoring and Diagnostic Engineering (COMADEM 2012)*, **364**: 012139, doi: 10.1088/1742-6596/364/1/012139.

2. Alfayez L., Mba D., Dyson G. (2005), The application of acoustic emission for detecting incipient cavitation and the best efficiency point of a 60kW centrifugal pump: Case study, *NDT & E International*, **38**(5): 354–358, doi: 10.1016/j.ndteint.2004.10.002.

3. Al-Obaidi A. (2018), *Experimental and Numerical Investigations on the Cavitation Phenomenon in a Centrifugal Pump*, Ph.D. Thesis, University of Huddersfield, UK.

4. Al-Obaidi A.R. (2019a), Experimental investigation of the effect of suction valve opening on the performance and detection of cavitation in the centrifugal pump based on acoustic analysis technique, *Archives of Acoustics*, **44**(1): 59–69, doi: 10.24425/aoa.2019. 126352.

5. Al-Obaidi A.R. (2019b), Monitoring the performance of centrifugal pump under single-phase and cavitation condition: A CFD analysis of the number of impeller blades, *Journal of Applied Fluid Mechanics*, **12**(2): 445–459, doi: 10.29252/JAFM.12.02.29303.

6. Anderson T. *et al.* (2014), *Introduction to Small Water Systems: A Course for Level 1 Operators*, Alaska, USA.

7. Arnold K., Stewart M. (1999), *Surface Production Operations, Design of Gas-Handling Systems and Facilities*, Vol. 2, Gulf Professional Publishing, Netherlands, doi: 10.1016/B978-0-88415-822-6.X5000-4.

8. Beebe R.S. (2004), *Predictive Maintenance of Pumps Using Condition Monitoring*, Elsevier, Netherlands.

9. Černetič J., Prezelj J., Čudina M. (2008), Use of noise and vibration signal for detection and monitoring of cavitation in kinetic pumps, *The Journal of the Acoustical Society of America*, **123**(5): 3316, doi: 10.1121/1.2933777.

10. Chudina M. (2003), Noise as an indicator of cavitation in a centrifugal pump, *Acoustical Physics*, **49**(4): 463–474, doi: 10.1134/1.1591303.

11. Čudina M. (2003), Detection of cavitation phenomenon in a centrifugal pump using audible sound, *Mechanical Systems and Signal Processing*, **17**(6): 1335–1347, doi: 10.1006/mssp.2002.1514.

12. Čudina M., Prezelj J. (2009), Detection of cavitation in operation of kinetic pumps. Use of discrete frequency tone in audible spectra, *Applied Acoustics*, **70**(4): 540–546, doi: 10.1016/j.apacoust.2008.07.005.

13. Farokhzad S., Bakhtyari N., Ahmadi H. (2013), Vibration signals analysis and condition monitoring of centrifugal pump, *Technical Journal of Engineering and Applied Sciences*, **4**: 1081–1085.

14. Gautam N. (2012), Construction working and advantages of centrifugal pump, *India Study Channel*, https://www.indiastudychannel.com/resources/149329-Construction-Working-And-Advantages-Of-Centrifugal-Pump.aspx.

15. Girdhar P., Moniz O. (2005), *Practical Centrifugal Pumps, Design, Operation and Maintenance*, Elsevier, Netherlands, doi: 10.1016/B978-0-7506-6273-4.X5000-4.

16. Grist E. (1998), *Cavitation and the Centrifugal Pump: A Guide for Pump Users*, Taylor & Francis, USA.

17. Jones G.M., Sanks R.L., Bosserman B.E., Tchobanoglous G. [Eds.] (2006), *Pumping Station Design*, Gulf Professional Publishing, USA.

18. Kamiel B.P (2015), Vibration-based Multi-fault Diagnosis for Centrifugal Pumps, Ph.D. Thesis, Curtin University.

19. Karassik I.J., McGuire T. (1998), *Centrifugal Pumps*, 2nd ed., Springer, USA.

20. Liu G. (2014), *Effects of Geometrical Parameters on Performance of Miniature Centrifugal Pump*, Ph.D. Thesis, Nanyang Technological University, Singapore.

21. Lobanoff V.S., Ross R.R (2013), *Centrifugal Pumps: Design and Application*, Elsevier, Netherlands.

22. Nelik L. (1999), *Centrifugal & Rotary Pumps: Fundamentals with Applications*, Taylor & Francis, USA.

23. Ramroop G., Liu K., Gu F., Payne B.S., Ball A.D. (2001), Airborne Acoustic Condition Monitoring of a Gearbox System, [in:] *2001 5th Annual Maintenance and Reliability Conference.*

24. Sakthivel N., Sugumaran V., Babudevasenapati S. (2010), Vibration based fault diagnosis of monoblock centrifugal pump using decision tree, *Expert Systems with Applications*, **37**(6): 4040–4049, doi: 10.1016/j.eswa.2009.10.002.

25. Spraker W.A. (1965), The effects of fluid properties on cavitation in centrifugal pumps, *Journal of Engineering for Gas Turbines and Power*, **87**(3): 309–318, doi: 10.1115/1.3678264.